High secretion of interferons by human plasmacytoid dendritic cells upon recognition of MERS-CoV

Vivian A. Scheuplein,[a] Janna Seifried,[a,e,*] Anna H. Malczyk,[a,f,*] Lilija Miller,[b] Lena Höcker,[b] Júlia Vergara-Alert,[c,h] Olga Dolnik,[c] Florian Zielecki,[c] Björn Becker,[d] Ingo Spreitzer,[d] Renate König,[e,f,g] Stephan Becker,[c,h] Zoe Waibler,[b,f,#] Michael D. Mühlebach[a,f,#]

Oncolytic Measles Viruses and Vaccine Vectors[a], Novel Vaccination Strategies and Early Immune Responses[b], Bacterial Safety[d], Host-Pathogen-Interactions[e], German Center for Infection Research[f], Paul-Ehrlich-Institut, Langen, Germany; Sanford-Burnham Medical Research Institute, Infectious & Inflammatory Disease Center, La Jolla, USA[g]; Institut für Virologie, Philipps-Universität Marburg, Marburg, Germany[c]; German Centre for Infection Research (DZIF), partner site Giessen-Marburg-Langen, Marburg, Germany[h]

Running title: MERS-CoV interacting with immune cells

#Address correspondence to
Dr. Michael Mühlebach, Michael.Muehlebach@pei.de; Dr. Zoe Waibler, Zoe.Waibler@pei.de

*J.S. and A.H.M. contributed equally to this work.

Word count abstract: 218 (abstract), 119 (importance)

Word count text: 5079

Abstract

The Middle East Respiratory Syndrome coronavirus (MERS-CoV) emerged in 2012 as causative agent of a severe respiratory disease with a fatality rate of approx. 30%. The high virulence and mortality rate prompted us to analyze aspects of MERS-CoV pathogenesis, especially its interaction with innate immune cells such as antigen-presenting cells (APCs). Particularly, we analyzed secretion of type I and type III interferons (IFNs) by APCs, i.e. B cells, macrophages, myeloid dendritic cells (MDDCs/mDCs), and by plasmacytoid dendritic cells (pDCs) of human and murine origin after inoculation with MERS-CoV. Production of high amounts of type I and III IFNs was induced exclusively in human pDCs, which was significantly higher than IFN induction by SARS-CoV. Of note, IFNs were secreted in absence of productive replication. However, receptor binding, endosomal uptake, and probably signaling via TLR7 were critical for sensing of MERS-CoV by pDCs. Furthermore, active transcription of MERS-CoV N RNA and subsequent N protein expression was evident in infected pDCs, indicating abortive infection. Taken together, our results point toward DPP4-dependent endosomal uptake and subsequent infection of human pDCs by MERS-CoV. However, the replication cycle is stopped after early gene expression. In parallel, human pDCs are potent IFN-producing cells upon MERS-CoV infection. Realization of such IFN responses supports understanding of MERS-CoV pathogenesis and is critical for the choice of treatment options.

Importance

MERS-CoV is causing a severe respiratory disease with high fatality rates in human patients. Recently, confirmed human cases have increased dramatically, both in number and geographic distribution. Understanding the pathogenesis of this highly pathogenic CoV is crucial for developing successful treatment strategies. This study elucidates the interaction of MERS-CoV

with APCs and pDCs particularly the induction of type I and III IFN secretion. Human pDCs are the immune cell population sensing MERS-CoV, but compared to SARS-CoV, secrete significantly higher amounts of IFNs, especially IFN-α. A model for molecular virus-host interactions is presented outlining IFN induction in pDCs. The massive IFN secretion upon contact suggests a critical role of this mechanism for the high immune activation observed during MERS-CoV infection.

Introduction

In 2012 a novel human betacoronavirus associated with severe respiratory disease emerged in Saudi Arabia (1). Due to its geographic distribution, this new virus was classified as Middle East Respiratory Syndrome coronavirus (MERS-CoV) (2). MERS-CoV is associated with high fatality rates (3, 4) and case numbers have globally increased to 909 laboratory confirmed cases with 331 fatalities (as of 21 November 2014, http://www.who.int/csr/don/21-november-2014-mers/en/). In parallel, the geographic distribution expands (4). MERS-CoV is the second emerging CoV with severe pathogenicity in humans within 10 years after the Severe Acute Respiratory Syndrome coronavirus (SARS-CoV) that infected approximately 8,000 people worldwide during its spread in 2003 (5). Human to human transmissions have been reported for MERS-CoV, but transmissibility seemed to be inefficient (6, 7). MERS-CoV persists in animal reservoirs, i.e. dromedary camels (8), and transmission events between camels and contact persons have been reported (7–10). Thus, MERS-CoV infection of men has zoonotic origins similar to SARS-CoV, but different to SARS-CoV, where bats have been identified as original virus reservoir, bats are discussed to host only closely related viruses of MERS-CoV (11). However, the only small animal model developed so far, are type I interferon receptor (IFNAR) deficient mice expressing human dipeptidyl peptidase 4 (DPP4, CD26), the entry receptor of MERS-CoV (12), in the lung after intranasal administration of huDPP4-expressing adenoviral vectors (13). MERS-CoV causes symptoms in humans similar to SARS-CoV such as severe pneumonia with acute respiratory distress syndrome, leukopenia and lymphopenia (14), septic shock, and multi-organ failure. A special feature of MERS-CoV infections are renal complications which may end in renal failure (15). The unusual tropism of MERS-CoV has been related to the wide tissue distribution of DPP4 e.g. on renal epithelial cells or leukocytes (16).

77 MERS-CoV replication is sensitive to type I and type III interferons (IFN) *in vitro* (17, 18) and
78 macaques can be protected by administration of IFN-β in combination with Ribavirin (19).
79 However, a benefit of IFN-β treatment could not be confirmed in 5 severely ill, presumably too
80 far progressed human patients (20, 21). Sensitivity of MERS-CoV to IFNs indicates that innate
81 immunity and IFN secretion are critical parameters for the outcome of MERS-CoV infection.
82 Type I IFNs, particularly IFN-β, can be produced by most stromal cell types upon viral infection.
83 Indeed, MERS-CoV actively suppresses type I IFN production in a variety of infected cell types
84 such as primary airway epithelial cells (18, 22). Additionally, professional antigen presenting
85 cells (APCs) are an important source of type I IFNs upon recognition of pathogen associated
86 molecular patterns (PAMPs) (23). Particularly plasmacytoid dendritic cells (pDCs) have been
87 shown to secrete high amounts of IFN-α after contact with virus (e.g. HIV-1 (24) or SARS-CoV
88 (25)). Type I IFNs have a significant bystander effect on uninfected neighboring cells by
89 inducing an antiviral state, activating innate immune cells, and priming adaptive immunity. On
90 the other hand, overshooting IFN-secretion can result in cytokine dysregulation and immune
91 pathogenesis (26).
92 To analyze the role of primary innate immune cells, especially their IFN secretion during MERS-
93 CoV infection, we inoculated a range of professional APCs and pDCs with MERS-CoV. No type
94 I or type III IFN was produced by murine mDCs, pDCs or peritoneal exudate cells (PECs) after
95 contact with MERS-CoV. Most interestingly, this was also the case for all human APC cell types,
96 which did not react to MERS-CoV with IFN secretion. Human pDCs, however, produced high
97 amounts of IFN-α and IFN-β, and moderate amounts of IFN-λ upon contact with MERS-CoV
98 without virus amplification. The observed IFN induction was dependent on availability of
99 MERS-CoV receptor DDP4, endosomal maturation, partially on PAMP recognition via TLR7
100 and correlated with *de novo* expression of MERS-CoV N protein. The high amounts of type I

IFNs which are secreted by pDCs during MERS-CoV infection suggest that type I IFNs hold a key position in MERS-CoV infection.

Materials and Methods

Cell lines and viruses. Vero cells (ATCC CCL-81) and BHK-21 cells [C-13] (ATCC CCL-10) were purchased from ATCC (Manassas, VA, USA) and cultured in DMEM (Lonza, Köln, Germany) supplemented with 2 mM glutamine and 10% FBS (Biochrome, Berlin, Germany) at 37°C in a humidified atmosphere containing 6% CO_2 for no longer than 6 months of culture after thawing of the original stock. MERS-CoV (EMC/2012) (14) and SARS-CoV (strain Frankfurt-1) (27) were propagated in Vero cells. Titers were determined by 50% tissue culture infection dose ($TCID_{50}$) titration on Vero cells (28). Virus stocks were stored in aliquots at -80°C. Inactivated MERS-CoV was generated by UV-inactivation (120,000 μJ/cm^2 UV light [254 nm], 90 min, Stratalinker UV Crosslinker, Stratagen, La Jolla, CA) of 0.1 ml virus suspension in 48 well plates on ice. Thogoto virus (THOV(ΔML)), an influenza-like orthomyxovirus inducing type I IFNs in murine mDCs (29), and Vesicular stomatitis virus M2 (VSV-M2) (30), a variant of VSV with defects in M protein functionality that induces high IFN responses in cells (31), were propagated on BHK-21 cells and titrated via plaque assay on Vero cells as described (30).

Isolation and generation of human professional antigen-presenting cells and pDCs. Human peripheral blood mononuclear cells (PBMCs) were isolated by Ficoll (Biochrom) density gradient centrifugation from buffy coats (Blutspendedienst, Frankfurt am Main, Germany) or citrate-blood of anonymized healthy human volunteers. Human B cells were purified by negative selection using the B-cell isolation kit II (Miltenyi Biotec, Bergisch Gladbach, Germany) and cultured as described before (32) and monocytes were purified by positive selection using CD14 MicroBeads (Miltenyi Biotec). For generation of monocyte-derived DC (MDDC), 2×10^5 $CD14^+$

monocytes were cultured in 96-well flat bottom tissue culture plates using X-VIVO 15 medium (Lonza) in the presence of GM-CSF (1000 U/ml; CellGenix, Freiburg, Germany) and IL-4 (1000 U/ml; CellGenix) for 5 days (33). For generation of GM-CSF-derived (M1) macrophages, monocytes were cultured in X-VIVO 15 medium supplemented with 10 ng/mL GM-CSF. For M-CSF-derived (M2) macrophage generation, monocytes were cultured in RPMI 1640 medium containing 10% FBS, 10 mM L-glutamine, 0.5 mM penicillin/streptomycin (PAA Laboratories, Egelsbach, Germany), 0.1 mM non-essential aminoacids (Biochrom) and 30 ng/mL M-CSF (R&D Systems, Wiesbaden-Nordendstadt, Germany) (34). Untouched human plasmacytoid dendritic cells (pDC) were isolated by negative selection from PBMCs using the Plasmacytoid Dendritic Cell Isolation Kit (Miltenyi Biotec) and cultured in RPMI 1640 (Biowest, Nuaillé, France) medium containing 10% FCS (Lonza), 10 mM L-glutamine and 100 ng/ml rec. IL-3 (R&D Systems). For subsequent experiments, all APCs were seeded in a density of $2.5x10^5$ APCs/well and pDCs were seeded in a density of $2x10^4$ pDCs/well in 96-well plates in 200 µl medium.

Generation of murine professional antigen-presenting cells. Murine bone marrow-derived myeloid dendritic cells (mDCs) and plasmacytoid dendritic cells (pDCs) were generated from bone marrow cells isolated from femurs and tibias of 6 to 10 weeks old C57BL/6N mice by differentiation with GM-CSF (R&D Systems) or Flt-3L (R&D Systems) for 8 days, as described before (35). Peritoneal exudate cells (PECs) were isolated from 6 to 10 weeks old C57BL/6N mice by flushing out cells from the abdominal cavity with 5 ml PBS and seeding 2×10^5 cells/ml in 200 µl RPMI 1640 (Biowest).

Virus growth kinetics. Vero cells, APCs, or pDCs were infected at an MOI of 0.01 or 5. Cells were washed once 1 h post infection, and incubated in respective cell culture media. At the

indicated time points, cell-free supernatants were sampled and stored at -80°C. Titers were determined by $TCID_{50}$ titration on Vero cells as described above.

Analysis of type I and III interferon secretion. Innate immune cells were inoculated with MERS-CoV, SARS-CoV, or UV-inactivated MERS-CoV. VSV-M2 (MOI = 0.1), THOV (MOI = 0.1), CpG 2216 [5 µg/ml], or CpG 2006 [5 µg/ml] (Invitrogen life technologies) (36) were used as controls. Cell-free supernatant was collected 24 hpi and stored at -80°C. Supernatants of human cells were analyzed for secreted IFNs using human IFN-α ELISA (Mabtech AB, Nacka Strand, Sweden), human IFN-β ELISA (R&D Systems), human IL-29 (IFN-λ1) ELISA (eBioscience, Frankfurt, Germany), or human IL-6 DuoSet ELISA development system (R&D Systems) according to manufacturers´ instructions. Supernatants of murine cells were analyzed using mouse IFN-α or mouse IFN-β ELISA (PBL Biomedical Laboratories, Piscataway, NJ) kits. To inhibit endosomal maturation or TLR7 signaling, pDCs were pre-incubated 30 min at 37°C with 5 µM chloroquine (Sigma) or 5.6 µM inhibitory oligonucleotide (ODN) IRS661 (Invitrogen life technologies), respectively, and infected with MERS-CoV (MOI = 1) in the presence of inhibitors. To inhibit receptor binding of MERS-CoV, pDCs were pre-incubated 30 min at 37°C with the recombinant receptor binding domain (RBD) 358-588 of MERS-CoV spike protein (S) or IgG1-Fc control protein [40 ng/ml] (37) before infection (MOI = 1).

Quantitative RT-PCR. $2x10^4$ pDCs were infected with MERS-CoV (MOI = 3) and washed once with medium 1 hpi. Total RNA of infected cells was isolated using the RNeasy plus mini kit (QIAgen) according to manufacturer´s instructions. 10 µl isolated RNA was reversely transcribed and quantified by qRT-PCR using SuperScript III Platinum OneStep qRT-PCR System (Invitrogen Life Technologies) with primers N2-Forward and N2-Reverse, and probe N2-Probe (labelled 5´ with 6-carboxyfluorescin and 3´ with Black Hole Quencher 1) as described (38) utilizing the ABI7900 HT Fast Real Time PCR System (Invitrogen Life technologies). The

amplification protocol was as follows: RT: 50°C for 30 min, Initial denaturation: 95°C for 2 min, PCR: 40 cycles of 95°C for 15 sec and 55°C for 1 min, Final elongation: 55°C for 5 min. Data were normalized to cellular GAPDH mRNA, which was quantified using SuperScript III Platinum SYBR Green OneStep qRT-PCR System (Invitrogen Life Technologies) with primers GapdH fwd (5´-GGCGATGCTGGCGCTGAGTAC-3´) and GapdH rev (5´-TGGTCCACACCCATGACGA-3´) for human GAPDH and mGAPDH fwd (5´-CACCAACTGCTTAGCCCC-3´) and mGAPDH rev (5´-TCTTCTGGGTGGCAGTGATG-3´) for murine GAPDH. The amplification protocol was as follows: 50°C for 30 min, 95°C for 15 min, 40 cycles of 94°C for 15 sec following 56°C for 1 min and 72°C for 30 sec, and 95°C for 15 min. The normalized Δc_t-value ($\Delta c_t = c_t$(MERS-vRNA) – c_t(GAPDH-mRNA)) thus describes the difference between threshold cycle numbers for qRT-PCR signals of viral RNA and cellular mRNA for a given sample. Therefore, the lower Δc_t, the higher is the relative amount of vRNA in the sample. Due to exponential amplification of DNA during PCR, differences (n) between Δc_t-values were converted to x-fold-ratios using the formula $x = 2^{-n}$, assuming optimal amplification for all samples.

Immunoblotting. For detection of CoV N-protein expression, $5x10^4$ pDCs were incubated with MERS-CoV (MOI = 3) and washed once with medium 1 hpi or 8 hpi. For blocking experiments, cells were pre-incubated with respective blocking agents as described above or with human DPPIV/CD26 Affinity Purified Polyclonal Ab (R&D Systems) or Goat IgG Control (R&D Systems) [40 µg/ml] (12) 30 min at 37°C before infection. Subsequently, washed pDCs were lysed and subjected to Immunoblot analysis as described (39). MERS-CoV N-protein was detected using a polyclonal rabbit anti-MERS-CoV serum (1:1,000) with donkey HRP-anti-rabbit IgG (H&L) (1:10,000) (Rockland, Gilbertsville, PA); β-actin was detected by mouse monoclonal anti-β-actin antibody (1:5,000, ab6276[AC-15], Abcam, Cambridge, UK) with HRP-rabbit anti-

mouse secondary antibody (Invitrogen life technologies). Pierce ECL 2 Western Blotting Substrate (Thermo Scientific) on Amersham Hyperfilm ECL (GE Healthcare) was used for detection of specific bands.

Flow cytometry analysis. Flow cytometry was performed on an LSRII-SORP FACS (BD, Heidelberg, Germany) and data were analyzed using the FACSDiva version 6.1.3 or FCS Express version 3 (De Novo Software, Los Angeles, CA). Cells were stained and analyzed as described before (39) using the following antibodies: mu α-hu CD26-PE (BA5b, Biolegend, San Diego, CA), mu α-hu CD14-FITC (M5E2, BD), mu α-hu CD19-PE (HIB19, BD Bioscience), mu α-hu CD123-PE (9F5, BD Bioscience), or mu α-hu DC303-APC (BD Bioscience) according to manufacturers´ instructions. Fc-block was performed with gammagard (Baxter, Deerfield, IL) [1,25 mg/ml]. Viability was checked by Fixable Viability Dye eFluor 780 (eBioscience).

Results

Analysis of type I IFN secretion in murine immune cells. Due to sensitivity of MERS-CoV to IFNs and the important role of innate immune cells in pathogen recognition and IFN secretion, we were interested in which innate immune cell subsets produce type I or type III IFNs upon contact with MERS-CoV. Therefore, type I IFN secretion by murine APCs and pDCs inoculated with MERS-CoV was analyzed first. Murine PECs (mainly macrophages), mDCs, or pDCs were inoculated with MERS- or SARS-CoV. For murine mDCs and PECs, THOV(ΔML) served as positive control for IFN secretion (29). Murine pDCs were inoculated with CpG2216 oligonucleotide to test the cells´ reactivity. All murine immune cells revealed robust IFN-α and IFN-β responses to the adequate positive controls, but no induction of type I IFN after contact with MERS-CoV or with SARS-CoV (Fig. 1A). Next, viral replication of MERS-CoV in murine

APCs was controlled, since inhibition of type I IFN production in MERS-CoV-infected cells has been described (17), potentially decoupling replication from IFN secretion. Productive viral replication in immune cells was quantified by titration of the supernatant of inoculated cells to detect released infectious progeny virus (Fig. 1B). Two days post infection, permissive Vero cells produced high peak titers of $5x10^6$ $TCID_{50}$/ml and $1x10^7$ $TCID_{50}$/ml of MERS- and SARS-CoV, respectively (Fig. 1B i). In contrast, no infectious virus considerably above the limit of detection ($1x10^2$ $TCID_{50}$/ml) was detected in the supernatants of any murine cell population for both MERS- and SARS-CoV (Fig. 1B ii).

Interferon production by human APCs upon contact with MERS-CoV. Although MERS-CoV did not induce any reactivity in murine immune cells, reactivity of human immune cells seemed not too unlikely, as SARS-CoV exhibited such pattern of IFN-induction (25). Therefore, we analyzed next, if and which human innate immune cell subset produces type I or type III IFNs upon inoculation with MERS-CoV. Human B cells, M1 and M2 type macrophages, MDDCs, and pDCs were inoculated with MERS-CoV or SARS-CoV. As positive controls for IFN secretion, M1 and M2 macrophages, and MDDCs were inoculated with VSV-M2 (30), B cells with the B cell stimulating CpG oligonucleotide CpG2006 (40), and pDCs with a pDC stimulating CpG oligonucleotide (41). Untreated cells served as mock control. Human B cells, M1 macrophages, M2 macrophages, or MDDCs did not secrete type I or type III IFNs upon inoculation with MERS-CoV, despite being responsive to appropriate stimuli (Fig. 2A). General responsiveness of B cells was confirmed by IL-6 secretion after stimulation with CpG2006 (Fig. 2D) (40). In contrast, human pDCs secreted high amounts of IFN-α, IFN-β, or IFN-λ (up to 40, 0.3, or 0.1 ng/ml, respectively) upon contact with MERS-CoV (Fig. 2A) with highest secretion at an intermediate MOI of 1. Interestingly, this did not correlate with rates of infection. pDCs inoculated with increasing MOIs of MERS-CoV revealed an approximately linear correlation of

viral RNA detectable in infected pDCs, as determined by calculating the normalized Δc_t values of qRT-PCR analysis and converting detected differences into fold-changes (Fig. 2B i-ii). These highest amounts of secreted IFNs at an MOI of 1 were about 8-, 4-, or 1.5-fold higher, respectively, than IFN levels measured after inoculation with SARS-CoV (5 ng/ml IFN-α, 0.07 ng/ml IFN-β, and 0.07 ng/ml IFN-λ). In addition, responses of human pDCs to CpG2216 (8.6 ng/ml IFN-α, 600 pg/ml IFN-β, and 80 pg/ml IFN-λ) were remarkably less strong than to MERS-CoV, but clearly detectable (41).

MERS-CoV replication in human innate immune cells. To analyze whether production of IFNs corresponds to productive replication of MERS-CoV in the respective human innate immune cell subsets, we inoculated cells with MERS-CoV and SARS-CoV at low MOI of 0.01. Productive viral replication was quantified by titration of the supernatant of inoculated cells to detect released infectious progeny virus (Fig. 2C). Similar to murine APCs (Fig. 1B ii) no infectious virus considerably above the limit of detection ($1x10^2$ $TCID_{50}$/ml) was detected in the supernatants of any human cell population for both MERS- and SARS-CoV (Fig. 2C). Thus, no productive replication of MERS-CoV in APCs and pDCs became evident after infection with low MOI. Since replication of MERS-CoV in M1 macrophages or MDDCs after high MOI infection has been published (42, 43), human pDCs were additionally infected at an MOI of 5 to test, if e.g putative anti-viral cellular restriction factors may be overcome by high MOI infection, and infectious virus in supernatants was titrated. A slowly decreasing titer with an initial set-point (1 hpi) of $2x10^4$ $TCID_{50}$/ml was detected in the supernatant (Fig. 2C ii). This indicates only inefficient replication of MERS-CoV in pDCs in our hands even after inoculation with high MOI. Thus, IFN secretion by pDCs is not linked to virus amplification.

Inhibition of IFN production by pDCs upon MERS-CoV contact. Next, we aimed to study the recognition of MERS-CoV in human pDCs. Therefore, human pDCs were inoculated with UV-

inactivated MERS-CoV particles (corresponding to an MOI of 1 before inactivation). UV-inactivated MERS-CoV induced secretion of similar amounts of IFN-α (50 ng/ml) and IFN-λ (0.06 ng/ml), but significantly reduced amounts of IFN-β (0.08 ng/ml) compared to untreated MERS-CoV (Fig. 3 i-iii). These results indicate the requirement for replication competent virus particles (even if no productive replication was evident in pDCs) to induce IFN-β secretion, whereas IFN-α and IFN-λ are induced by replication-defective virus particles as well, as evident by similar differences between UV-inactivated and untreated MERS-CoV compared to mock.

To determine the route of MERS-CoV cell entry necessary for viral replication, we first analyzed the role of the virus receptor DPP4. Analysis of DPP4 surface expression by flow cytometry indicated surface expression of DPP4 on human pDCs (Fig. 4A). Indeed, pre-incubation of human pDCs with the receptor binding domain (RBD) of MERS-CoV (37) to block active MERS-CoV entry reduced secretion of IFNs by pDCs. Secretion of IFN-α was reduced 10-fold (3 ng/ml *vs.* 30 ng/ml), IFN-β 26-fold (0.03 ng/ml vs. 0.8 ng/ml), but IFN-λ only slightly (37 pg/ml vs. 43 pg/ml) compared to control-treated cells (Fig. 3 iv-vi). For IFN-λ the impact of 1 outliner data point with high IFN-λ secretion within this experiment influenced the data. In an additional dataset RBD blocked IFN-λ, again, for each of the 3 studied donors (Suppl. Fig. 1 iii). However, also after stimulation by CpG2216 the secretion of all IFNs was strongly reduced in the presence of RBD protein (1.5 vs. 150 ng/ml IFN-α, less 50 pg/ml vs 0.16 ng/ml IFN-β, 4 pg/ml vs. 40 pg/ml IFN-λ) indicating general immune suppressive properties of the RBD protein (Fig. 4C).

To evaluate if MERS-CoV particles are endocytosed and if MERS-CoV is recognized in the endosome, endosomal maturation and thus, the endosomal route of entry and IFN induction (44)

were inhibited by chloroquine. Of note, 24 h after co-treatment with chloroquine or RBD and MERS-CoV, viability of pDCs was not impaired (Fig. 4B i-ii). When pDCs were infected with MERS-CoV (MOI = 1) in the presence of chloroquine, the secretion of IFNs was reduced by a factor of 11 for IFN-α (5 ng/ml vs. 55 ng/ml), 35 for IFN-β (0.6 ng/ml vs. 0.016 ng/ml), and 2.3 for IFN-λ (60 pg/ml vs. 140 pg/ml) (Fig. 3 vii-ix). These data indicate that the endosomal route is critical for sensing of MERS-CoV infection by human pDCs. Since viral RNA can be recognized as PAMP in the endosomes of pDCs by TLR7, we inhibited TLR7 via the inhibitory ODN IRS661. IFN-α production was 1.5-fold decreased upon TLR7-inhibition (15 ng/ml vs. 25 ng/ml) compared to infection in the presence of a non-inhibiting control oligonucleotide. IFN-β production was 3-fold decreased (0.25 ng/ml vs. 0.73 ng/ml) and IFN-λ production was 2-fold decreased upon TLR7-inhibition (36 pg/ml vs. 77 pg/ml) (Fig. 3 x-xii). Thus, secretion of all IFNs analyzed was reduced upon inhibition of TLR7. These data indicate involvement of TLR7 in sensing MERS-CoV RNA and in IFN-induction upon MERS-CoV infection of pDCs.

Transcription of MERS-CoV N RNA in infected pDCs. Even though no significant productive viral replication was observed, initial steps of viral infection and replication may take place in pDCs and could be responsible for triggering cytosolic pattern recognition receptors (PRRs). To analyze MERS-CoV infection of pDCs, onset of viral transcription was monitored by qRT-PCR of N protein RNA in infected pDCs. For this purpose, total RNA of human pDCs infected with MERS-CoV (MOI = 3) was isolated and amounts of MERS-CoV N RNA was quantified 1 hpi and 6 hpi and normalized to cellular housekeeping gene mRNA (GAPDH) (Fig. 5A). The relative amount of N RNA increases from 1 hpi to 6 hpi by 14-fold indicating onset of viral gene transcription. In line with IFN-blocking experiments, only minimal increase in relative N RNA levels were detected when human pDCs were pretreated with chloroqine (1.2-fold) or when murine pDCs were used as substrate (no increase) (Fig 5A).

Expression of MERS-CoV nucleocapsid protein in infected human pDCs. To back up mRNA expression data, the onset of viral protein translation was monitored by immunoblot analysis of viral N protein expression in infected pDCs. For this purpose, human pDCs were infected with MERS-CoV (MOI = 3) and N protein expression was checked (Fig. 5C-D). As expected, no CoV N protein was detected in murine pDCs (Fig. 5B) and human pDCs 1 hpi (Fig. 5C-D). However, 8 hpi CoV-N protein expression was clearly demonstrated in human pDCs, indicating onset of viral gene expression in infected human pDCs. In contrast, using polyclonal DPP4 antibody or the RBD, MERS-CoV N protein expression was decreased in comparison to the respective control indicating infection of pDCs via DPP4 (Fig. 5C). Moreover, when human pDCs were inoculated with UV-inactivated MERS-CoV, no expression of N protein was detected, thus indicating that intact viral genomes are crucial for N protein expression (Fig. 5D). In addition, inhibition of endosomal maturation was accompanied by considerably less N protein expression in infected cells 8 hpi (Fig. 5D). Therefore, expression of MERS-CoV N depends on receptor binding and endosomal maturation arguing for the endosomal pathway as primary route of MERS-CoV entry into human pDCs.

Discussion

Our data reveal that primary human pDCs produce high amounts of type I and type III IFN in response to MERS-CoV infection. Sensing depends on receptor availability, endosomal uptake, and at least partially functionality of TLR7. Moreover, we detected expression of MERS-CoV N mRNA and protein in the absence of progeny virus, suggesting unproductive infection of human pDCs. Similar to data obtained upon SARS-CoV infection, secretion of IFNs was exclusively found in pDCs (25) but amounts of IFNs induced by MERS-CoV were significantly higher.

In parallel, stimulation with CpG2216 resulted also in lower, but clearly detectable amounts of IFNs. Thereby, integrity of pDCs can be assumed, since the amount of secreted IFNs were comparable to previously published data (25, 41) considering the fact, that only a third of pDCs was used and IFN-containing supernatants were harvested after 24 h, here.

When human B cells, macrophages, or MDDCs were inoculated with MERS-CoV, no type I or III IFNs were detected in the supernatant of infected cells. In line with these data, Zhou *et al*. (42) could not detect upregulation of type I IFN mRNA upon infection of human macrophages. Also in infected human MDDCs, only minor induction of IFN-α mRNA and no induction of IFN-β mRNA synthesis were detected (43).

In contrast, high amounts of IFN-α were detected when human pDCs were inoculated with MERS-CoV. IFN-α can be induced in pDCs after recognition of PAMPs in the endosome e.g. via TLR7 (45). In our experiments, secretion of IFN-α was strongly inhibited by chloroquine treatment. Indeed, chloroquine is an inhibitor of endosomal maturation and can inhibit IFN production induced by viruses (e.g. HIV) via PRRs within the endosome (46). When the endosomal PRR of pDCs for viral RNA, TLR7, was inhibited, secretion of IFN-α also decreased. Taken together, these data argue for endosomal recognition of MERS-CoV, potentially recognition via TLR7, in mature endosomes of pDCs. The pattern of IFN-λ secretion by human pDCs after MERS-CoV inoculation was following IFN-α, as expected, since IFN-λ is induced by similar stimuli as IFN-α (47).

IFN-β was also secreted in significant amounts by human pDCs upon MERS-CoV inoculation. IFN-β can be induced after recognition of PAMPs by cytosolic PRRs such as MDA-5 or RIG-I (48). Indeed, we demonstrated the onset of viral gene expression in human pDCs. In line, UV inactivation of MERS-CoV, which damages the viral genome and thereby inhibits transcription

and amplification of viral RNA, significantly reduced IFN-β secretion, but secretion of IFN-α or IFN-λ remained on a similar level. Thus, cytoplasmic recognition of viral replication intermediates seems to be responsible for IFN-β induction. However, MERS-CoV-induced IFN-β secretion was also blocked by chloroquine, an effect that cannot be explained when postulating direct viral entry across the plasma membrane after contact of the viral spike glycoprotein S with its receptor CD26/DDP4, as assumed for MERS-CoV entry into lung epithelial cells (49). To use this entry pathway, MERS-CoV-S has to be activated by cellular exopeptidases; mainly transmembrane protease serine 2 (TMPRSS2) has been demonstrated to be responsible for cleavage during MERS-CoV entry into Calu-3 cells (49). In contrast, we demonstrate that endosomal maturation is crucial for MERS-CoV entry into pDCs. Interestingly, uptake of MERS-CoV via the endosomal route has already been described as an alternative pathway for entry into e.g. Vero cells (49). Here, lysosomal proteases such as cathepsin L are required to activate the MERS-CoV-S protein (50), but their activity depends on endosomal maturation (51). Hence, chloroquine-mediated inhibition of IFN-β secretion by pDCs after contact with MERS-CoV argues for receptor-mediated endocytosis of MERS-CoV particles and activation of MERS-CoV-S protein by endosomal proteases such as cathepsin L finally resulting in cytosolic entry of MERS-CoV across the endosomal membrane. Indeed, expression of mRNA and MERS-CoV-N protein was considerably decreased in presence of chloroquine, indicating chloroquine-mediated inhibition of infection.

Furthermore, we blocked cell attachment of MERS-CoV to pDCs by blocking DPP4 with recombinant viral RBD. Block of receptor binding led to significant reduction of IFN production following virus inoculation. However, CpG-stimulated IFN-induction was blocked by recombinant RBD as well, indicating immune suppressive properties of the MERS-CoV RBD in human pDCs. DPP4 is described as an activating receptor on T lymphocytes (52–54) but its

386 function in DCs has only been linked to T cell stimulation, yet (55). Thus the reasons for
387 eventually immune-suppressive properties of the RBD domain remain to be elucidated.
388 Nevertheless, the remarkable inhibition of N protein expression by both RBD and αDPP4 serum
389 indicate the necessity of DPP4 as entry receptor for endocytotic uptake and subsequent infection
390 on human pDCs. Receptor-dependent endocytosis as uptake-pathway for MERS-CoV may also
391 explain the absence of IFN-induction in murine pDCs after contact with the virus. In contrast to
392 human DPP4, murine DPP4 is no suitable receptor for promoting infection with MERS-CoV
393 (56). Thus, lack of binding of MERS-CoV to murine DPP4 should reduce endosomal uptake of
394 virus particles, thereby reducing the amount of PAMPs which can be sensed by PRRs, resulting
395 in strongly reduced IFN induction in murine pDCs.
396 To summarize the data, a model explaining the mechanism how MERS-CoV induces type I IFN
397 in human pDCs may be proposed (Fig. 6). MERS-CoV binds to its entry receptor DPP4 on the
398 surface of pDCs triggering receptor-mediated endocytosis of viral particles. In the mature
399 endosome, MERS-CoV RNA is sensed by TLR7 inducing IFN-α secretion. Furthermore, MERS-
400 CoV spike proteins become cleaved by endosomal proteases during or after endosome
401 maturation. This cleavage allows fusion of viral and endosomal membranes causing release of the
402 viral genome into the cytoplasm. In the cytoplasm, expression of viral proteins starts. We
403 hypothesize that MERS-CoV RNA replication intermediates are recognized by cytosolic PRRs
404 resulting in full-blown induction of IFN-β. However, assembly or release of new progeny viral
405 particles is impaired by yet unknown mechanisms in stages subsequent to viral gene expression.
406 This absence of significant MERS-CoV replication in pDCs contrasting the virus´ replication in
407 MDDCs (43) or macrophages (42) may be explained by the significant (biological and
408 functional) differences also to other DC subsets (58). In line with this hypothesis, also influenza

409 A virus replication was demonstrated in mDCs, but shown to be blocked at post-entry steps in
410 pDCs (59).
411 Apart from being crucial for MERS-CoV recognition by pDCs, lack of functional entry receptors
412 in mice leads to lack of IFN production in murine cells. Meanwhile, it has been shown that
413 murine DPP4 cannot be used as MERS-CoV entry receptor, as demonstrated by expression of
414 human DDP4 in mouse lungs via adenoviral vectors, this is sufficient to gain (partial)
415 susceptibility to MERS-CoV infection (13).
416 Moreover, type I (57) and type III (17) IFNs inhibit MERS-CoV replication *in vitro*. A
417 characteristic feature of type I IFNs is that effects are seen at small concentrations. In this
418 previous studies replication of MERS-CoV was inhibited by type I and III IFN in different cell
419 types *in vitro* already starting at ng/ml concentration range (17, 57, 60). The IFN-α levels
420 obtained in the experiments met such amounts at least 40-fold, thus, the amounts of IFNs
421 produced by pDCs upon MERS-CoV infection can be supposed to be relevant. Thus, release of
422 type I and III IFNs may protect against MERS-CoV-induced pathogenicity. It is therefore
423 counterintuitive that MERS-CoV induces significantly higher secretion of IFN than SARS-CoV
424 when infecting pDCs, but clinically recorded MERS patients having a worse prognosis than
425 SARS patients had (5). However, secretion of extraordinary high amounts of type I IFNs can
426 result in aberrant immune activation. Zhou *et al.* already speculated that an induced cytokine
427 storm could be the reason for the severity of illness on the basis of high amounts of pro-
428 inflammatory cytokines and chemokines such as IL-12 or IP-10 secreted by human macrophages
429 upon MERS-CoV infection (42). In human SARS patients, aberrant IFN-stimulated gene
430 expression and cytokine responses compared to healthy individuals were indeed observed (61).
431 Patients that had such kind of hyper-immune activation succumbed more likely to the infection
432 (62). Furthermore, the severity of SARS correlated with high amounts of inflammatory cytokines

in serum (63), and symptoms of disease became usually worse after virus clearance (64). For these reasons, immune-mediated pathogenesis has been proposed for SARS-CoV infection (62). If such a pathomechanism may also apply to MERS and pDCs are really the major source of IFNs in such a setting remains to be demonstrated in further studies. However, the up to 8-fold enhanced IFN type I secretion upon MERS-CoV infection compared to SARS-CoV might hint at overshooting immune reactions being potentially one factor for the higher mortality rate observed in MERS patients, then.

Acknowledgements

The authors would like to thank Heike Schmitz, Steffen Prüfer, Stefanie Bauer, and Christiane Tondera for excellent technical assistance, and Kay-Martin Hanschmann for statistical analysis. The authors are indebted to Dr. Ron Fouchier for providing MERS-CoV strain EMC/2012, to Dr. Christian Drosten and Dr. Doreen Muth for SARS-CoV strain Frankfurt-1 and PCR-protocols, and to Dr. Berend Jan Bosch for MERS-CoV RBD and control IgG1 Fc protein.

References

1. **Bermingham A, Chand MA, Brown CS, Aarons E, Tong C, Langrish C, Hoschler K, Brown K, Galiano M, Myers R, Pebody RG, Green HK, Boddington NL, Gopal R, Price N, Newsholme W, Drosten C, Fouchier RA, Zambon M.** 2012. Severe respiratory illness caused by a novel coronavirus, in a patient transferred to the United Kingdom from the Middle East, September 2012. Euro Surveill. **17**:20290.
2. **Groot RJ de, Baker SC, Baric RS, Brown CS, Drosten C, Enjuanes L, Fouchier RAM, Galiano M, Gorbalenya AE, Memish ZA, Perlman S, Poon LLM, Snijder EJ, Stephens GM, Woo PCY, Zaki AM, Zambon M, Ziebuhr J.** 2013. Middle East respiratory

syndrome coronavirus (MERS-CoV): announcement of the Coronavirus Study Group. J. Virol. **87**:7790–7792. doi:10.1128/JVI.01244-13.

3. **van Boheemen S, Graaf M de, Lauber C, Bestebroer TM, Raj VS, Zaki AM, Osterhaus ADME, Haagmans BL, Gorbalenya AE, Snijder EJ, Fouchier RAM.** 2012. Genomic characterization of a newly discovered coronavirus associated with acute respiratory distress syndrome in humans. MBio **3. doi:**10.1128/mBio.00473-12.

4. **Al-Tawfiq JA, Memish ZA.** 2014. Middle East respiratory syndrome coronavirus: epidemiology and disease control measures. Infection and drug resistance **7**:281–287. doi:10.2147/IDR.S51283.

5. **Peiris, J S M, Guan Y, Yuen KY.** 2004. Severe acute respiratory syndrome. Nat. Med. **10**:S88-97. doi:10.1038/nm1143.

6. **Breban R, Riou J, Fontanet A.** 2013. Interhuman transmissibility of Middle East respiratory syndrome coronavirus: estimation of pandemic risk. Lancet **382**:694–699. doi:10.1016/S0140-6736(13)61492-0.

7. **Drosten C, Meyer B, Müller MA, Corman VM, Al-Masri M, Hossain R, Madani H, Sieberg A, Bosch BJ, Lattwein E, Alhakeem RF, Assiri AM, Hajomar W, Albarrak AM, Al-Tawfiq JA, Zumla AI, Memish ZA.** 2014. Transmission of MERS-coronavirus in household contacts. The New England journal of medicine **371**:828–835. doi:10.1056/NEJMoa1405858.

8. **Haagmans BL, Al Dhahiry, Said H S, Reusken, Chantal B E M, Raj VS, Galiano M, Myers R, Godeke G, Jonges M, Farag E, Diab A, Ghobashy H, Alhajri F, Al-Thani M, Al-Marri SA, Al Romaihi, Hamad E, Al Khal A, Bermingham A, Osterhaus, Albert D M E, Alhajri MM, Koopmans, Marion P G.** 2014. Middle East respiratory syndrome

479 coronavirus in dromedary camels: an outbreak investigation. Lancet Infect Dis **14**:140–145.
480 doi:10.1016/S1473-3099(13)70690-X.
481 9. **Azhar EI, El-Kafrawy SA, Farraj SA, Hassan AM, Al-Saeed MS, Hashem AM, Madani**
482 **TA.** 2014. Evidence for camel-to-human transmission of MERS coronavirus. The New
483 England journal of medicine **370**:2499–2505. doi:10.1056/NEJMoa1401505.
484 10. **Madani TA, Azhar EI, Hashem AM.** 2014. Evidence for camel-to-human transmission of
485 MERS coronavirus. The New England journal of medicine **371**:1360.
486 doi:10.1056/NEJMc1409847.
487 11. **Corman VM, Ithete NL, Richards LR, Schoeman MC, Preiser W, Drosten C, Drexler**
488 **JF.** 2014. Rooting the phylogenetic tree of middle East respiratory syndrome coronavirus by
489 characterization of a conspecific virus from an african bat. J. Virol. **88**:11297–11303.
490 doi:10.1128/JVI.01498-14.
491 12. **Raj VS, Mou H, Smits SL, Dekkers DHW, Müller MA, Dijkman R, Muth D, Demmers**
492 **JAA, Zaki A, Fouchier RAM, Thiel V, Drosten C, Rottier PJM, Osterhaus ADME,**
493 **Bosch BJ, Haagmans BL.** 2013. Dipeptidyl peptidase 4 is a functional receptor for the
494 emerging human coronavirus-EMC. Nature **495**:251–254. doi:10.1038/nature12005.
495 13. **Zhao J, Li K, Wohlford-Lenane C, Agnihothram SS, Fett C, Zhao J, Gale MJ, Baric**
496 **RS, Enjuanes L, Gallagher T, McCray PB, Perlman S.** 2014. Rapid generation of a
497 mouse model for Middle East respiratory syndrome. Proc. Natl. Acad. Sci. U.S.A.
498 **111**:4970–4975. doi:10.1073/pnas.1323279111.
499 14. **Zaki AM, van Boheemen S, Bestebroer TM, Osterhaus ADME, Fouchier RAM.** 2012.
500 Isolation of a novel coronavirus from a man with pneumonia in Saudi Arabia. N. Engl. J.
501 Med. **367**:1814–1820. doi:10.1056/NEJMoa1211721.

15. **Drosten C, Seilmaier M, Corman VM, Hartmann W, Scheible G, Sack S, Guggemos W, Kallies R, Muth D, Junglen S, Müller MA, Haas W, Guberina H, Röhnisch T, Schmid-Wendtner M, Aldabbagh S, Dittmer U, Gold H, Graf P, Bonin F, Rambaut A, Wendtner C.** 2013. Clinical features and virological analysis of a case of Middle East respiratory syndrome coronavirus infection. Lancet Infect Dis **13**:745–751. doi:10.1016/S1473-3099(13)70154-3.

16. **Schütz F, Hackstein H.** 2014. Identification of novel dendritic cell subset markers in human blood. Biochem. Biophys. Res. Commun. **443**:453–457. doi:10.1016/j.bbrc.2013.11.112.

17. **Kindler E, Jónsdóttir HR, Muth D, Hamming OJ, Hartmann R, Rodriguez R, Geffers R, Fouchier RAM, Drosten C, Müller MA, Dijkman R, Thiel V.** 2013. Efficient replication of the novel human betacoronavirus EMC on primary human epithelium highlights its zoonotic potential. MBio **4**:e00611-12. doi:10.1128/mBio.00611-12.

18. **Zielecki F, Weber M, Eickmann M, Spiegelberg L, Zaki AM, Matrosovich M, Becker S, Weber F.** 2013. Human cell tropism and innate immune system interactions of human respiratory coronavirus EMC compared to those of severe acute respiratory syndrome coronavirus. J. Virol. **87**:5300–5304. doi:10.1128/JVI.03496-12.

19. **Falzarano D, Wit E de, Rasmussen AL, Feldmann F, Okumura A, Scott DP, Brining D, Bushmaker T, Martellaro C, Baseler L, Benecke AG, Katze MG, Munster VJ, Feldmann H.** 2013. Treatment with interferon-α2b and ribavirin improves outcome in MERS-CoV-infected rhesus macaques. Nat. Med. **19**:1313–1317. doi:10.1038/nm.3362.

20. **Al-Tawfiq JA, Momattin H, Dib J, Memish ZA.** 2014. Ribavirin and interferon therapy in patients infected with the Middle East respiratory syndrome coronavirus: an observational study. Int. J. Infect. Dis. doi:10.1016/j.ijid.2013.12.003.

21. **Khalid M, Al Rabiah F, Khan B, Al Mobeireek A, Butt TS, Al Mutairy E.** 2014. Ribavirin and interferon (IFN)-alpha-2b as primary and preventive treatment for Middle East respiratory syndrome coronavirus (MERS-CoV): a preliminary report of two cases. Antiviral therapy. doi:10.3851/IMP2792.

22. **Chan RWY, Chan MCW, Agnihothram S, Chan LLY, Kuok DIT, Fong JHM, Guan Y, Poon LLM, Baric RS, Nicholls JM, Peiris JSM.** 2013. Tropism of and innate immune responses to the novel human betacoronavirus lineage C virus in human ex vivo respiratory organ cultures. J. Virol. **87**:6604–6614. doi:10.1128/JVI.00009-13.

23. **Siegal FP, Kadowaki N, Shodell M, Fitzgerald-Bocarsly PA, Shah K, Ho S, Antonenko S, Liu YJ.** 1999. The nature of the principal type 1 interferon-producing cells in human blood. Science **284**:1835–1837.

24. **Beignon A, McKenna K, Skoberne M, Manches O, DaSilva I, Kavanagh DG, Larsson M, Gorelick RJ, Lifson JD, Bhardwaj N.** 2005. Endocytosis of HIV-1 activates plasmacytoid dendritic cells via Toll-like receptor-viral RNA interactions. J. Clin. Invest. **115**:3265–3275. doi:10.1172/JCI26032.

25. **Cervantes-Barragan L, Züst R, Weber F, Spiegel M, Lang KS, Akira S, Thiel V, Ludewig B.** 2007. Control of coronavirus infection through plasmacytoid dendritic-cell-derived type I interferon. Blood **109**:1131–1137. doi:10.1182/blood-2006-05-023770.

26. **Haller O, Kochs G, Weber F.** 2006. The interferon response circuit: induction and suppression by pathogenic viruses. Virology **344**:119–130. doi:10.1016/j.virol.2005.09.024.

27. **Drosten C, Günther S, Preiser W, van der Werf, Sylvie, Brodt H, Becker S, Rabenau H, Panning M, Kolesnikova L, Fouchier, Ron A M, Berger A, Burguière A, Cinatl J, Eickmann M, Escriou N, Grywna K, Kramme S, Manuguerra J, Müller S, Rickerts V, Stürmer M, Vieth S, Klenk H, Osterhaus, Albert D M E, Schmitz H, Doerr HW.** 2003.

549 Identification of a novel coronavirus in patients with severe acute respiratory syndrome. N.
550 Engl. J. Med. **348**:1967–1976. doi:10.1056/NEJMoa030747.
551 28. **Kärber G.** 1931. Beitrag zur kollektiven Behandlung pharmakologischer Reihenversuche.
552 Arch Exp Pathol Pharmakol:480–483.
553 29. **Kochs G, Bauer S, Vogt C, Frenz T, Tschopp J, Kalinke U, Waibler Z.** 2010. Thogoto
554 virus infection induces sustained type I interferon responses that depend on RIG-I-like
555 helicase signaling of conventional dendritic cells. J. Virol. **84**:12344–12350.
556 doi:10.1128/JVI.00931-10.
557 30. **Waibler Z, Detje CN, Bell JC, Kalinke U.** 2007. Matrix protein mediated shutdown of host
558 cell metabolism limits vesicular stomatitis virus-induced interferon-alpha responses to
559 plasmacytoid dendritic cells. Immunobiology **212**:887–894.
560 doi:10.1016/j.imbio.2007.09.003.
561 31. **Stojdl DF, Lichty BD, tenOever BR, Paterson JM, Power AT, Knowles S, Marius R,**
562 **Reynard J, Poliquin L, Atkins H, Brown EG, Durbin RK, Durbin JE, Hiscott J, Bell**
563 **JC.** 2003. VSV strains with defects in their ability to shutdown innate immunity are potent
564 systemic anti-cancer agents. Cancer Cell **4**:263–275. doi:10.1016/S1535-6108(03)00241-1.
565 32. **Weissmüller S, Semmler LY, Kalinke U, Christians S, Müller-Berghaus J, Waibler Z.**
566 2012. ICOS-LICOS interaction is critically involved in TGN1412-mediated T-cell
567 activation. Blood **119**:6268–6277. doi:10.1182/blood-2011-12-401083.
568 33. **Sender LY, Gibbert K, Suezer Y, Radeke HH, Kalinke U, Waibler Z.** 2010. CD40
569 ligand-triggered human dendritic cells mount interleukin-23 responses that are further
570 enhanced by danger signals. Mol. Immunol. **47**:1255–1261.
571 doi:10.1016/j.molimm.2009.12.008.

34. **Neu C, Sedlag A, Bayer C, Förster S, Crauwels P, Niess J, van Zandbergen G, Frascaroli G, Riedel CU.** 2013. CD14-dependent monocyte isolation enhances phagocytosis of listeria monocytogenes by proinflammatory, GM-CSF-derived macrophages. PLoS ONE **8**:e66898. doi:10.1371/journal.pone.0066898.

35. **Waibler Z, Anzaghe M, Ludwig H, Akira S, Weiss S, Sutter G, Kalinke U.** 2007. Modified vaccinia virus Ankara induces Toll-like receptor-independent type I interferon responses. J. Virol. **81**:12102–12110. doi:10.1128/JVI.01190-07.

36. **Kerkmann M, Rothenfusser S, Hornung V, Towarowski A, Wagner M, Sarris A, Giese T, Endres S, Hartmann G.** 2003. Activation with CpG-A and CpG-B oligonucleotides reveals two distinct regulatory pathways of type I IFN synthesis in human plasmacytoid dendritic cells. J. Immunol. **170**:4465–4474.

37. **Mou H, Raj VS, van Kuppeveld, Frank J M, Rottier, Peter J M, Haagmans BL, Bosch BJ.** 2013. The receptor binding domain of the new Middle East respiratory syndrome coronavirus maps to a 231-residue region in the spike protein that efficiently elicits neutralizing antibodies. J. Virol. **87**:9379–9383. doi:10.1128/JVI.01277-13.

38. **Lu X, Whitaker B, Sakthivel, Senthil Kumar K, Kamili S, Rose LE, Lowe L, Mohareb E, Elassal EM, Al-sanouri T, Haddadin A, Erdman DD.** 2014. Real-time reverse transcription-PCR assay panel for Middle East respiratory syndrome coronavirus. J. Clin. Microbiol. **52**:67–75. doi:10.1128/JCM.02533-13.

39. **Funke S, Maisner A, Mühlebach MD, Koehl U, Grez M, Cattaneo R, Cichutek K, Buchholz CJ.** 2008. Targeted cell entry of lentiviral vectors. Mol. Ther. **16**:1427–1436. doi:10.1038/mt.2008.128.

40. **Hartmann G, Krieg AM.** 2000. Mechanism and function of a newly identified CpG DNA motif in human primary B cells. J. Immunol. **164**:944–953.

41. **Krug A, Rothenfusser S, Hornung V, Jahrsdörfer B, Blackwell S, Ballas ZK, Endres S, Krieg AM, Hartmann G.** 2001. Identification of CpG oligonucleotide sequences with high induction of IFN-alpha/beta in plasmacytoid dendritic cells. Eur. J. Immunol. **31**:2154–2163. doi:10.1002/1521-4141(200107)31:7<2154:AID-IMMU2154>3.0.CO;2-U.

42. **Zhou J, Chu H, Li C, Wong BH, Cheng Z, Poon VK, Sun T, Lau CC, Wong KK, Chan JY, Chan JF, To KK, Chan K, Zheng B, Yuen K.** 2013. Active Replication of Middle East Respiratory Syndrome Coronavirus Replication and Aberrant Induction of Inflammatory Cytokines and Chemokines in Human Macrophages: Implications for Pathogenesis. J. Infect. Dis. doi:10.1093/infdis/jit504.

43. **Chu H, Zhou J, Wong BH, Li C, Cheng Z, Lin X, Poon VK, Sun T, Lau CC, Chan JF, To KK, Chan K, Lu L, Zheng B, Yuen K.** 2014. Productive replication of Middle East respiratory syndrome coronavirus in monocyte-derived dendritic cells modulates innate immune response. Virology **454-455**:197–205. doi:10.1016/j.virol.2014.02.018.

44. **Lee J, Chuang T, Redecke V, She L, Pitha PM, Carson DA, Raz E, Cottam HB.** 2003. Molecular basis for the immunostimulatory activity of guanine nucleoside analogs: activation of Toll-like receptor 7. Proc. Natl. Acad. Sci. U.S.A. **100**:6646–6651. doi:10.1073/pnas.0631696100.

45. **Birmachu W, Gleason RM, Bulbulian BJ, Riter CL, Vasilakos JP, Lipson KE, Nikolsky Y.** 2007. Transcriptional networks in plasmacytoid dendritic cells stimulated with synthetic TLR 7 agonists. BMC Immunol. **8**:26. doi:10.1186/1471-2172-8-26.

46. **Martinson JA, Montoya CJ, Usuga X, Ronquillo R, Landay AL, Desai SN.** 2010. Chloroquine modulates HIV-1-induced plasmacytoid dendritic cell alpha interferon: implication for T-cell activation. Antimicrob. Agents Chemother. **54**:871–881. doi:10.1128/AAC.01246-09.

47. **Coccia EM, Severa M, Giacomini E, Monneron D, Remoli ME, Julkunen I, Cella M, Lande R, Uzé G.** 2004. Viral infection and Toll-like receptor agonists induce a differential expression of type I and lambda interferons in human plasmacytoid and monocyte-derived dendritic cells. Eur. J. Immunol. **34**:796–805. doi:10.1002/eji.200324610.

48. **Li J, Liu Y, Zhang X.** 2010. Murine coronavirus induces type I interferon in oligodendrocytes through recognition by RIG-I and MDA5. J. Virol. **84**:6472–6482. doi:10.1128/JVI.00016-10.

49. **Shirato K, Kawase M, Matsuyama S.** 2013. Middle East respiratory syndrome coronavirus infection mediated by the transmembrane serine protease TMPRSS2. J. Virol. **87**:12552–12561. doi:10.1128/JVI.01890-13.

50. **Gierer S, Bertram S, Kaup F, Wrensch F, Heurich A, Krämer-Kühl A, Welsch K, Winkler M, Meyer B, Drosten C, Dittmer U, Hahn T von, Simmons G, Hofmann H, Pöhlmann S.** 2013. The spike protein of the emerging betacoronavirus EMC uses a novel coronavirus receptor for entry, can be activated by TMPRSS2, and is targeted by neutralizing antibodies. J. Virol. **87**:5502–5511. doi:10.1128/JVI.00128-13.

51. **Guha S, Padh H.** 2008. Cathepsins: fundamental effectors of endolysosomal proteolysis. Indian J. Biochem. Biophys. **45**:75–90.

52. **Dong RP, Kameoka J, Hegen M, Tanaka T, Xu Y, Schlossman SF, Morimoto C.** 1996. Characterization of adenosine deaminase binding to human CD26 on T cells and its biologic role in immune response. Journal of immunology (Baltimore, Md. : 1950) **156**:1349–1355.

53. **Ohnuma K, Dang NH, Morimoto C.** 2008. Revisiting an old acquaintance: CD26 and its molecular mechanisms in T cell function. Trends in immunology **29**:295–301. doi:10.1016/j.it.2008.02.010.

643 54. **Dang NH, Torimoto Y, Deusch K, Schlossman SF, Morimoto C.** 1990. Comitogenic
644 effect of solid-phase immobilized anti-1F7 on human CD4 T cell activation via CD3 and
645 CD2 pathways. Journal of immunology (Baltimore, Md. : 1950) **144**:4092–4100.
646 55. **Zhong J, Rao X, Deiuliis J, Braunstein Z, Narula V, Hazey J, Mikami D, Needleman B,**
647 **Satoskar AR, Rajagopalan S.** 2013. A potential role for dendritic cell/macrophage-
648 expressing DPP4 in obesity-induced visceral inflammation. Diabetes **62**:149–157.
649 doi:10.2337/db12-0230.
650 56. **Cockrell AS, Peck KM, Yount BL, Agnihothram SS, Scobey T, Curnes NR, Baric RS,**
651 **Heise MT.** 2014. Mouse dipeptidyl peptidase 4 is not a functional receptor for Middle East
652 respiratory syndrome coronavirus infection. J. Virol. **88**:5195–5199. doi:10.1128/JVI.03764-
653 13.
654 57. **Falzarano D, Wit E de, Martellaro C, Callison J, Munster VJ, Feldmann H.** 2013.
655 Inhibition of novel β coronavirus replication by a combination of interferon-α2b and
656 ribavirin. Sci Rep **3**:1686. doi:10.1038/srep01686.
657 58. **Dalod M, Chelbi R, Malissen B, Lawrence T.** 2014. Dendritic cell maturation: functional
658 specialization through signaling specificity and transcriptional programming. The EMBO
659 journal **33**:1104–1116. doi:10.1002/embj.201488027.
660 59. **Smed-Sörensen A, Chalouni C, Chatterjee B, Cohn L, Blattmann P, Nakamura N,**
661 **Delamarre L, Mellman I.** 2012. Influenza A virus infection of human primary dendritic
662 cells impairs their ability to cross-present antigen to CD8 T cells. PLoS pathogens
663 **8**:e1002572. doi:10.1371/journal.ppat.1002572.
664 60. **Hart BJ, Dyall J, Postnikova E, Zhou H, Kindrachuk J, Johnson RF, Olinger GG,**
665 **Frieman MB, Holbrook MR, Jahrling PB, Hensley L.** 2014. Interferon-β and

mycophenolic acid are potent inhibitors of Middle East respiratory syndrome coronavirus in cell-based assays. J. Gen. Virol. **95**:571–577. doi:10.1099/vir.0.061911-0.

61. **Huang K, Su I, Theron M, Wu Y, Lai S, Liu C, Lei H.** 2005. An interferon-gamma-related cytokine storm in SARS patients. J. Med. Virol. **75**:185–194. doi:10.1002/jmv.20255.

62. **Cameron MJ, Ran L, Xu L, Danesh A, Bermejo-Martin JF, Cameron CM, Muller MP, Gold WL, Richardson SE, Poutanen SM, Willey BM, DeVries ME, Fang Y, Seneviratne C, Bosinger SE, Persad D, Wilkinson P, Greller LD, Somogyi R, Humar A, Keshavjee S, Louie M, Loeb MB, Brunton J, McGeer AJ, Kelvin DJ.** 2007. Interferon-mediated immunopathological events are associated with atypical innate and adaptive immune responses in patients with severe acute respiratory syndrome. J. Virol. **81**:8692–8706. doi:10.1128/JVI.00527-07.

63. **Wong CK, Lam, C W K, Wu, A K L, Ip WK, Lee, N L S, Chan, I H S, Lit, L C W, Hui, D S C, Chan, M H M, Chung, S S C, Sung, J J Y.** 2004. Plasma inflammatory cytokines and chemokines in severe acute respiratory syndrome. Clin. Exp. Immunol. **136**:95–103. doi:10.1111/j.1365-2249.2004.02415.x.

64. **Perlman S, Dandekar AA.** 2005. Immunopathogenesis of coronavirus infections: implications for SARS. Nat. Rev. Immunol. **5**:917–927. doi:10.1038/nri1732.

Figure Legends

Fig. 1. Inoculation of murine cells with MERS-CoV. (A) Type I IFN secretion by murine immune cells. Cells were inoculated with MERS-CoV (MOIs as indicated), SARS-CoV, or indicated positive controls. Single dots, individual experiments; horizontal line, mean. IFNs were measured 24 hpi. b.d.: below detection; Limits of detection: IFN-α, 12.5 pg/ml; IFN-β, 15.6

pg/ml. (B) growth kinetics of MERS-CoV on (i) Vero cells or (ii) murine APCs (MOI = 0.01). Indicated cell types were inoculated with virus and sampled supernatants were titrated. Filled: MERS-CoV, open: SARS-CoV. ◊, PEC; ○, mDCs; □, pDCs. Mean of 3 independent experiments; error bars, standard deviation..

Fig. 2. Inoculation of human immune cells with MERS-CoV. (A) Type-I and -III IFN secretion by human immune cells. Human cells were inoculated with MERS-CoV (MOIs indicated), SARS-CoV (MOI = 1), or indicated positive controls (CpG2006, VSV-M2 or CpG2216). Supernatants were sampled 24 hpi and secreted IFNs were determined by specific ELISAs. (B) Isolated RNA was used for qRT-PCR. MERS-RNA signals were normalized to cellular GAPDH mRNA (Δc_t = ct(MERS-RNA) – c_t(GAPDH mRNA)). (i) Δc_t values and (ii) respectively calculated x-fold amounts of RNA normalized to MOI 0.1. (C) Titers of MERS-CoV or SARS-CoV (control) in (i) human immune cells infected at an MOI of 0.01 or (ii) on pDCs infected at an MOI of 5. (D) IL-6 secretion by human B cells upon inoculation with stimulating CpG2006. Supernatants were sampled 24 h after inoculation with CpG2006 and secreted IFNs were determined by ELISA. Individual donors are displayed as single dots and horizontal lines indicate mean. b.d., below detection; limits of detection: IFN-α, 7 pg/ml; IFN-β, 50 pg/ml; IFN-λ, 8 pg/ml. *, $P < 0.05$. Filled: MERS-CoV, open: SARS-CoV. ◊, B cells/PEC; Δ, M1-macrophages; ∇, M2-macrophages; ○, MDDCs; □, pDCs. Growths in Vero cells (left), in human APCs (MOI = 0.01) (middle), or in human pDCs (MOI = 5) (right). Mean of 3 independent experiments; error bars, standard deviation.

Fig. 3. Dissecting type I and III IFN induction in human pDCs. . Impact of different parameters on IFN-induction in pDCs after inoculation of MERS-CoV (MOI = 1): (i-iii) Live

714 virus; pDCs were incubated with UV-inactivated virus (UV), or live virus (MERS-CoV). (iv-ix)
715 Entry receptor; infection in the presence or absence of (iv-vi) MERS-CoV-S receptor binding
716 domain (RBD) or IgG1-Fc control protein (Ctrl). (vii-ix) Endosomal maturation; infection in the
717 presence of chloroquine. (x-xii) TLR recognition; infection in the presence of TLR7 inhibitor
718 (IRS 661). IFNs were sampled 24 hpi. Mock and MERS-CoV data for live virus experiments are
719 same as displayed in Fig. 1. Individual donors: single dots, horizontal line: mean. ns, not
720 significant; *, $P < 0.05$; **, $P < 0.01$.
721
722 **Fig. 4. CD26 expression and functionality of human pDCs.** (A) Expression of MERS-CoV
723 receptor DPP4 on human pDCs. pDCs were stained with aDPP4 antibody and analyzed via flow
724 cytometry. (B) Viability of pDCs of 3 different donors (D1-3) treated with inhibitors. pDCs were
725 treated as indicated. 24 hpi, cells were stained for viability and analyzed via flow cytometry. (C)
726 Block of CpG2216-induced IFN secretion by MERS-CoV RBD. Secretion of indicated IFNs in
727 the presence or absence of MERS-CoV-S receptor binding domain (RBD) or IgG1-Fc control
728 protein (Ctrl) upon MERS-CoV infection or DPP4-independent stimulus CpG2216. IFNs were
729 sampled 24 hpi. Individual donors: single dots, horizontal line: mean. b.d., below detection.
730
731 **Fig. 5. Infection of human pDCs by MERS-CoV.** (A) Quantification of viral N RNA in human
732 or murine pDCs by qRT-PCR in the presence or absence of chloroquine, normalized to cellular
733 GAPDH mRNA (Δc_t = c_t(MERS-vRNA) – c_t(GAPDH-mRNA)) at indicated time points after
734 inoculation. (B-D) Immunoblot analysis of N protein expression in (B) murine pDCs or (C-D)
735 human pDCs after inoculation with MERS-CoV (MOI = 3). pDCs of 3 different donors (D1-D3
736 and D4-D6) were infected in presence of blocking α-DPP4 serum (DPP4), the receptor binding
737 domain of MERS-CoV S protein (RBD), or respective controls (Ctrl) (C) or with UV-inactivated

(UV) or live MERS-CoV in the presence (Chl) or absence (sham) of chloroquine (D). Cells were lysed at indicated time points and subjected to analyses.

Fig. 6. Model for MERS-CoV induced type I IFN secretion in human pDCs. The figure schematically depicts the life-cycle of MERS-CoV in human pDCs and events triggering secretion or infection of type I IFNs. Successful inhibition of IFN secretion at single steps is indicated. Inhibitors or proteins which have been analyzed are depicted in bold. Question marks point out steps during assembly or release of viral particles the block of which could be responsible for absence of significant viral replication in pDCs.

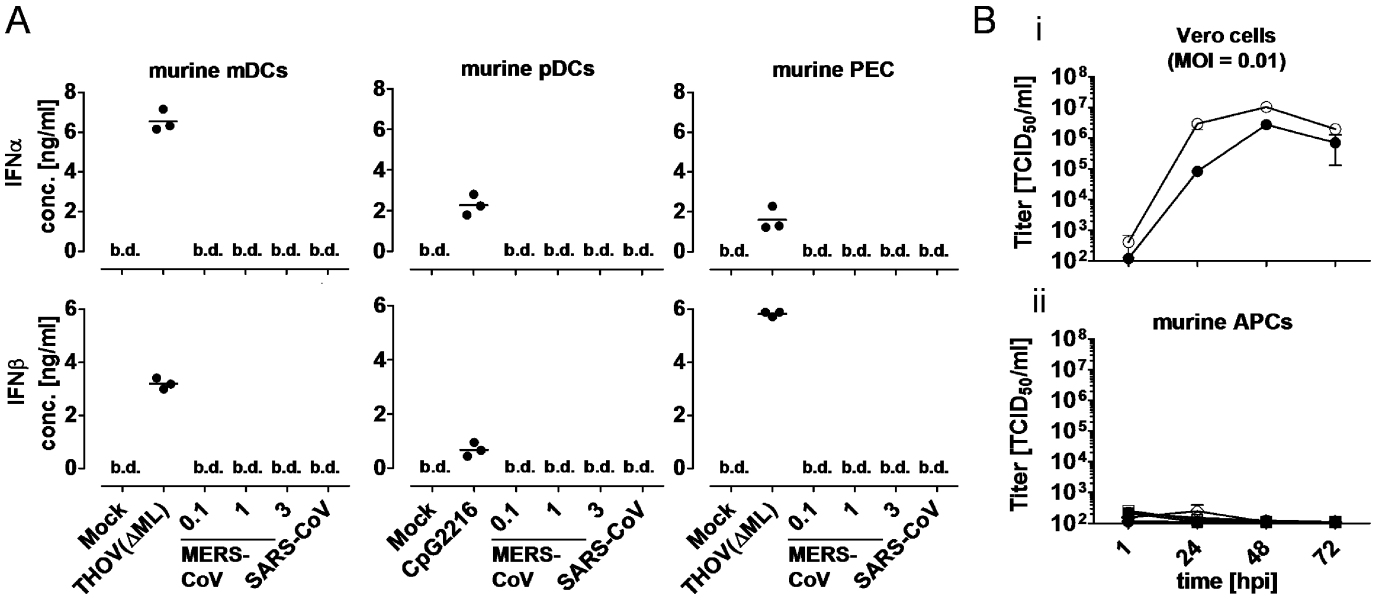

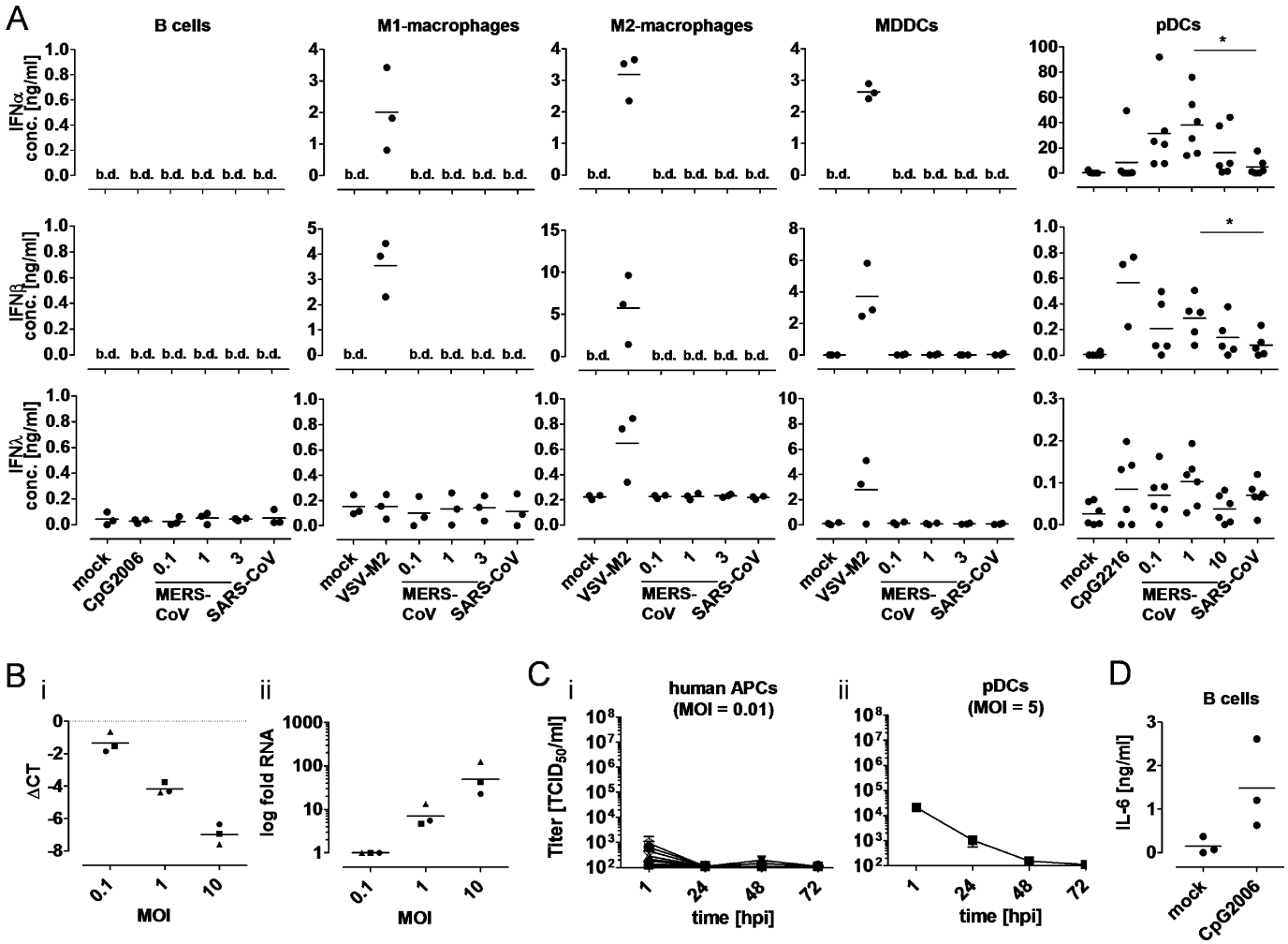

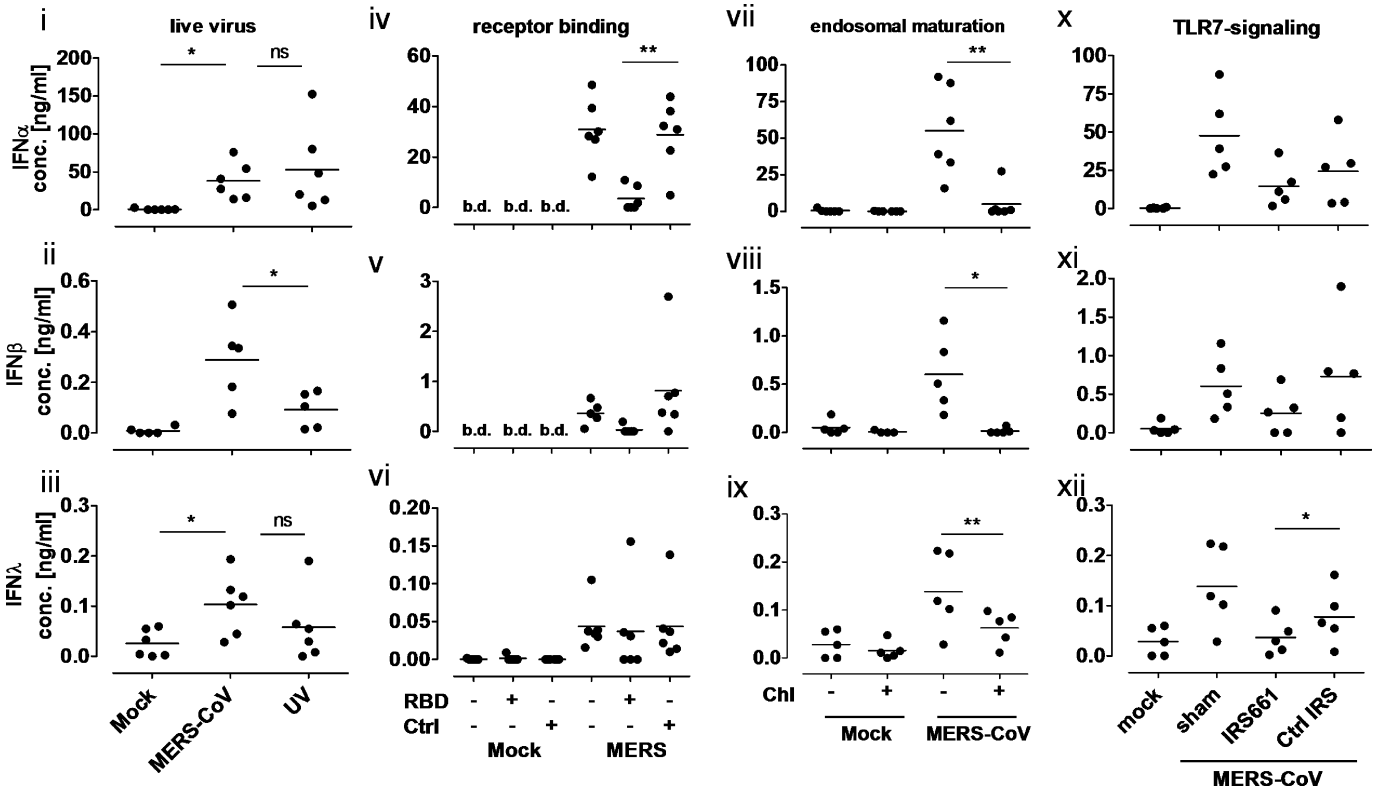

Journal of Virology